

XRD Studies on Titanium Substituted Manganese -Zinc Ferrite System, $Mn_{0.8+x}Zn_{0.2}Ti_xFe_{2-2x}O_4$ with $x=0.10, 0.15, 0.20$

Satheesh D J¹, Vasudevan Nair N², Jayakumari Isac^{3*}

¹Centre for Condensed Matter, Department of Physics, CMS college, Kottayam, India

²Department of Physics, M. G College, Trivandrum, Kerala.

^{3*}Department of Physics, CMS college, Kottayam, 686001, India

Keywords: MnZnFeTiO, XRD, SEM, EDX, Instrumental Broadening, Williamson-Hall Plot method.

Abstract. $Mn_{0.8+x}Zn_{0.2}Ti_xFe_{2-2x}O_4$ where $x=0.1, 0.15, 0.20$ were prepared by conventional solid state reaction technique starting with AR grade MnO, ZnO, TiO₂ and Fe₂O₃. Final sintering was done at 1150°C for 20 hours followed by slow cooling to room temperature. The sample was analyzed by X-ray Diffraction (XRD), Particle size determination, SEM and EDX. The comparison of XRD results with JCPDS files confirmed the single phase spinel structure. Scanning Electron Microscopy (SEM) studies revealed that the average grain size of samples as 10µm. EDX spectrum shows the elements of the sample. X-ray instrumental broadening analysis was used to evaluate the size and lattice strain by the Williamson-Hall Plot method.

1. Introduction

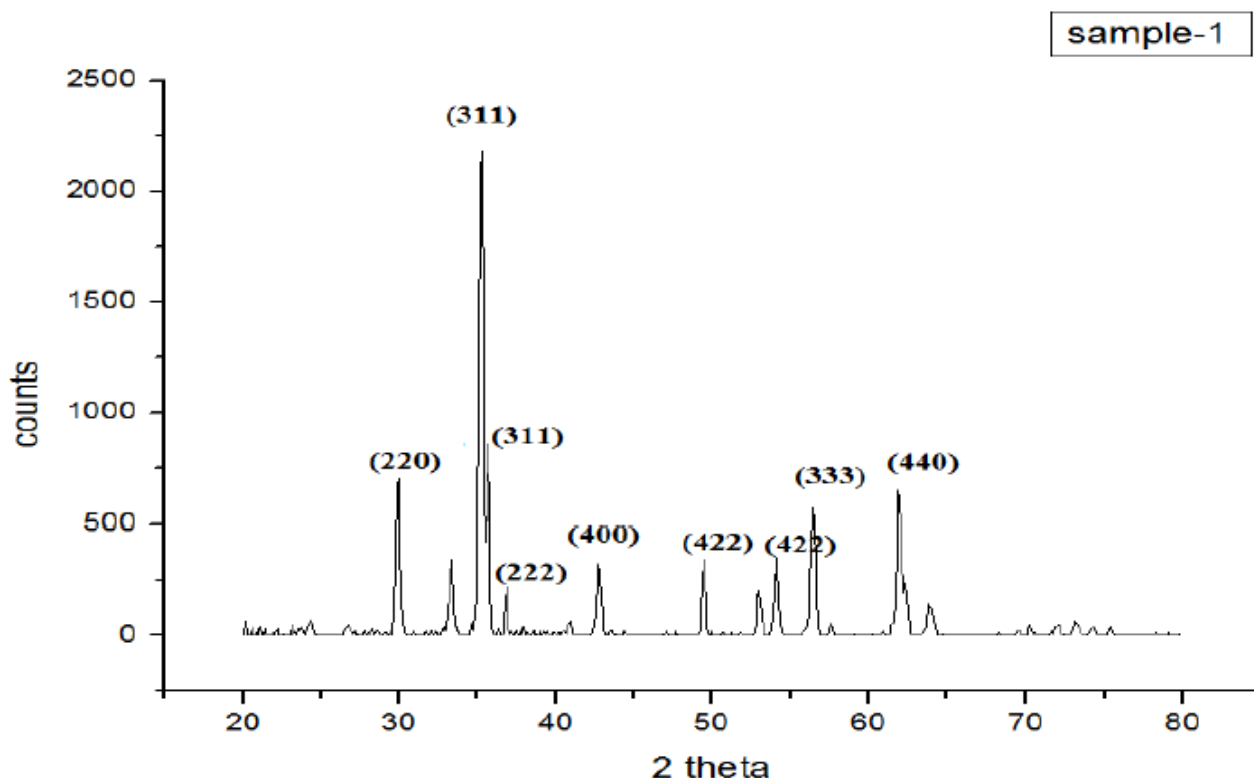
Ferrites are ferromagnetic semi conductors and the need for high resistivity ferrites led to the synthesis of various ferrites. The influence of various substituent like Ti, Zn etc considerably change in its electrical properties[1]. Polycrystalline ferrites have very good dielectric properties [2]. Ferrites having very high dielectric constants are useful in designing good microwave devices such as isolators, circulators etc. Manganese-Zinc Ferrite $Mn_{0.8+x}Zn_{0.2}Fe_2O_4$ in the spinel structure is a low cost material which is generally useful for microwave - devices and memory-core applications. Due to Ti substitution electrical and magnetic properties changes and hence have much technological merits [3,4,5]. In this work the authors describe the preparation of $Mn_{0.8+x}Zn_{0.2}Ti_xFe_{2-2x}O_4$ with $x=0.10, 0.15, 0.20$ and characterized to show good quality and homogeneity. The results were analyzed by X-ray Diffraction (XRD), SEM, EDX. The particle size was determined from XRD details. The EDX Spectrum gave the information on the elemental composition of the material. The particle size and strain of the material was found by Instrumental Broadening and Williamson-Hall Plot method.

2. Materials and Experimental Methods

The ferrite samples having the compositional formula $Mn_{0.8+x}Zn_{0.2}Ti_xFe_{2-2x}O_4$ where $x=0.1, 0.15, 0.2$ were prepared by solid state reaction method. The initial ingredients MnO, ZnO, TiO₂, Fe₂O₃ were weighed and mixed in correct Stoichiometric ratio and grounded for ten hours using an agate mortar. The resulting mixture was air dried and presintered in air for 10 hours at 700°C. Temperature is controlled by a platinum-Rhodium thermocouple within the furnace. The presintered ferrites were then again grounded for two to three hours. The granulated powder was then pressed into pellets and toroids at a pressure of 1N/M² with the help of hydraulic press. The binder used was polyvinyl alcohol solution. The final sintering was done at 1150°C for 20 hours followed by slow cooling to room temperature. Chopper stabilized amplifier is used as temperature control system within the furnace. Phase identification is done by XRD. Scanning Electron Microscopy (SEM) was taken for experimental confirmation of the calculated particle size. From EDX, the composition details of the prepared samples were determined.

2.1. XRD Analysis.

XRD Diffraction pattern for the three samples ($x=0.1, 0.15, 0.2$) of $Mn_{0.8+x}Zn_{0.2}Ti_xFe_{2-2x}O_4$ was taken using Bruker AXS D8 advance diffractometer (figure 1). The diffractometer with radiations of wavelength 1.54060\AA having Nickel filter equipped with X-ray generator 1140/90/96 having X-ray source KRISTALLOFLXE 780, KF,4KE with wide angle goniometer PW 3050/60 with single pen recorder pm 8203 and channel control PW1390 at 40 KV, 30mA at measurement temperature of 25°C is used for the purpose. The scanning speed of the specimen is 2 degree / minute.



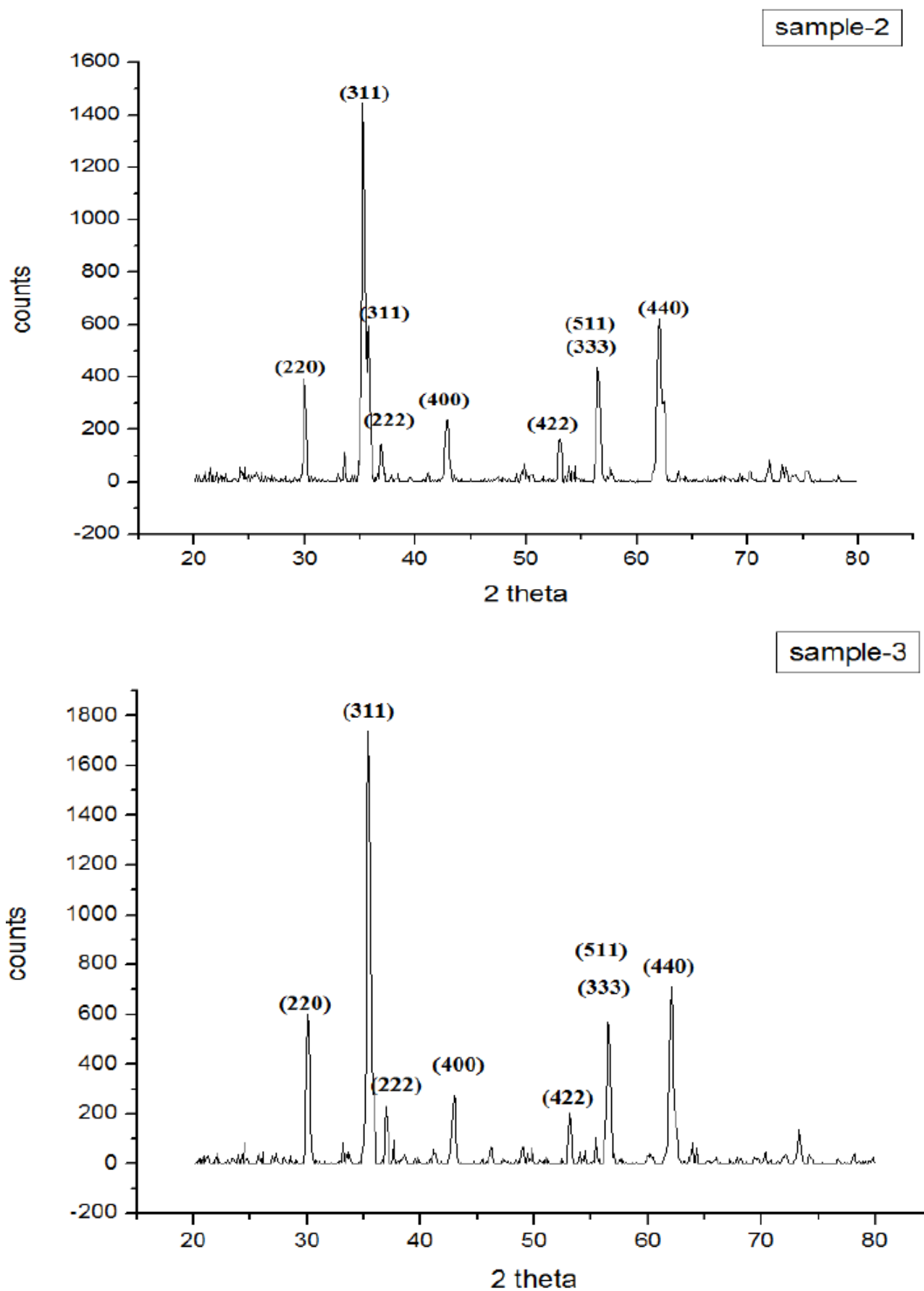


Fig 1. XRD of $Mn_{0.8+x}Zn_2Ti_xFe_{2-2x}O_4$ for $x=0.1, 0.15, 0.20$ (sample 1, 2, 3)

From the XRD results, the obtained peaks are matching with the JCPDS file values with card No.742402. Hence these samples are of single phase spinel structure with $a = b = c = 8.445$ Å and $\alpha = \beta = \gamma = 90^\circ$. The lattice parameters of three samples have been calculated using d spacing. A plot of lattice parameter against titanium content is shown on figure(2). It shows that lattice parameter varies with titanium concentration. Titanium is doped in place of Fe^{3+} . When majority of Fe^{3+} in octahedral site is replaced by Ti^{3+} the lattice parameter can increase and when majority of Fe^{3+} is replaced by Ti^{4+} the lattice parameter can decrease [6].

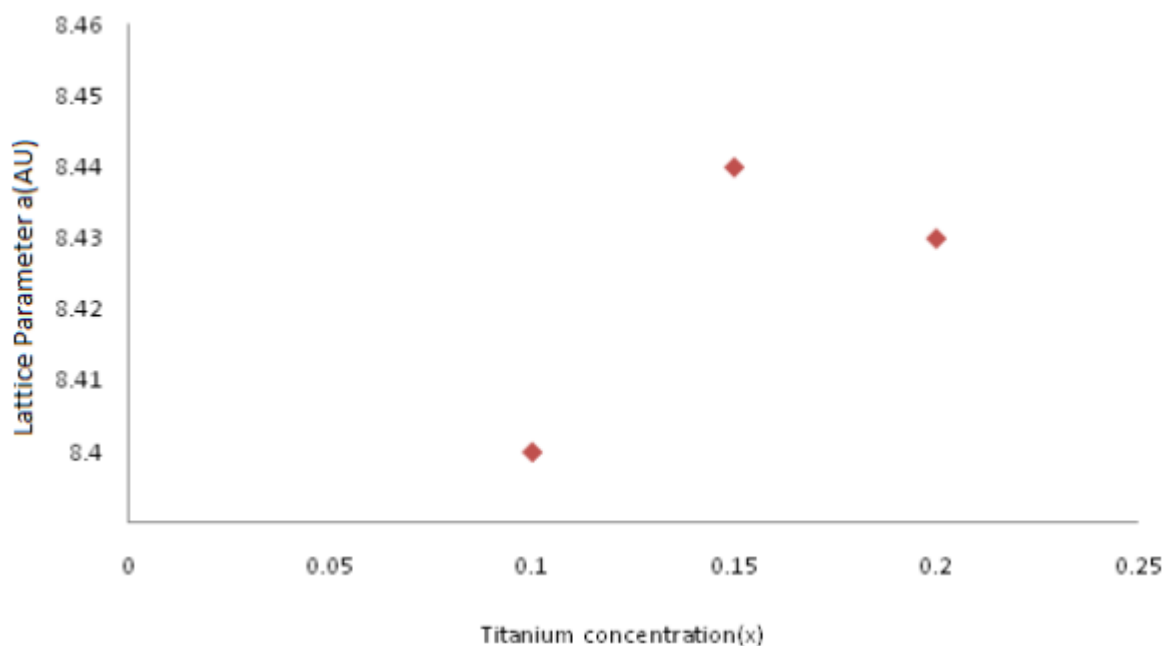


Fig 2. Lattice parameter against titanium content

2.2 Particle Size Measurements.

Crystal structures are solved by analyzing the intensities of different X-ray beams. X-ray diffraction profile may be used to find the average crystal size in the sample. The broadening of the diffraction lines than usual decreases with the increase in particle size.

The Debye Scherrer equation for calculating the particle size is given by.

$$D = \frac{K\lambda}{\beta \cos\theta} \quad (7)$$

Where K is the Scherrer constant, λ is the wavelength of light used for the diffraction, β is the full width at half maximum of the sharp peaks and θ is the angle measured. The Scherrer constant (K) in the above formula accounts for the shape of the particle and is generally taken to have the value 0.9.

2.3 XRD- Instrumental Broadening.

Diffraction pattern will show broadening because of particle size and strain. The observed line broadening (figure 3) is used to estimate the average size of the particles. Sample broadening is described by

$$FW(s) \times \cos \theta = \frac{K\lambda}{\text{size}} + 4 \times \text{strain} \times \sin \theta$$

The total broadening β_t is found as,

$$\beta_t^2 \approx \left\{ \frac{0.9\lambda}{D \cos \theta} \right\}^2 + \{4\varepsilon \tan \theta\}^2 + \beta_0^2$$

Where D is average particle size, ε is strain and β_0 is instrumental broadening.

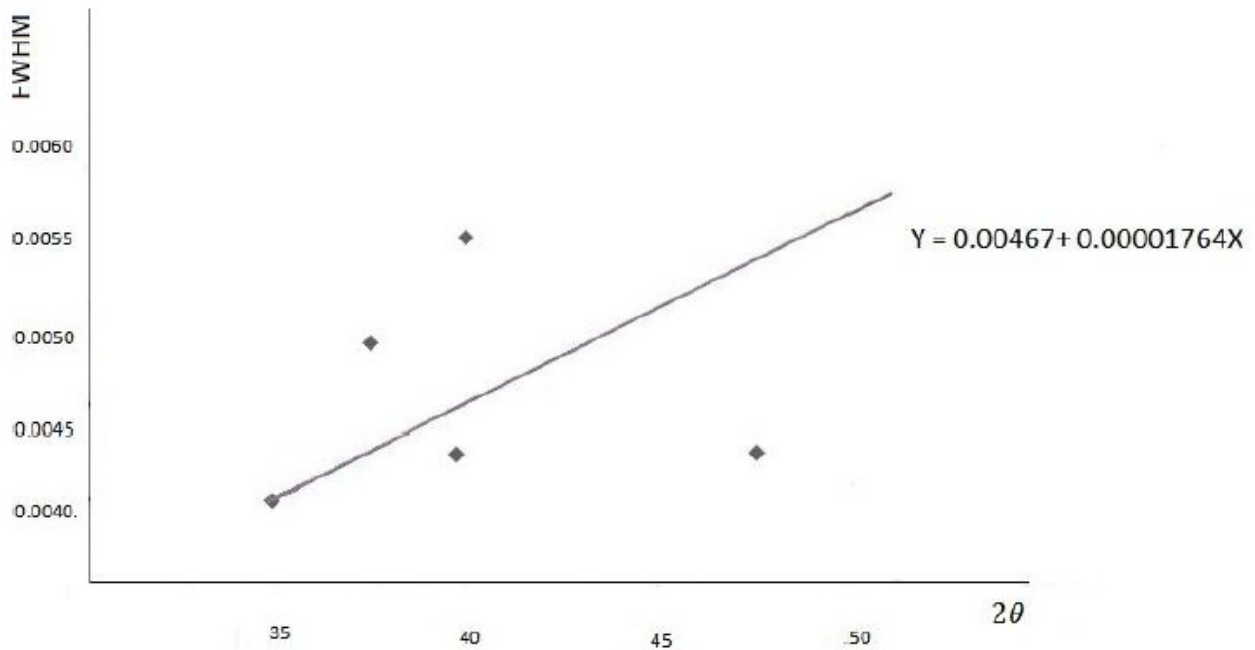


Fig 3. Typical instrumental broadening.

2.4 Williamson-Hall plot

G.K. Williamson and his student W.H Hall were developed this method. The principle behind is that the approximate formulae for size broadening β_L and strain broadening β_e vary quite differently with respect to Bragg angle θ . Williamson and Hall proposed a method for deconvoluting size and strain broadening by looking at the peak width as a function of 2θ . [8].

$$\beta_L = \frac{K\lambda}{L \cos \theta}$$

$$\beta_e = C\varepsilon \tan \theta$$

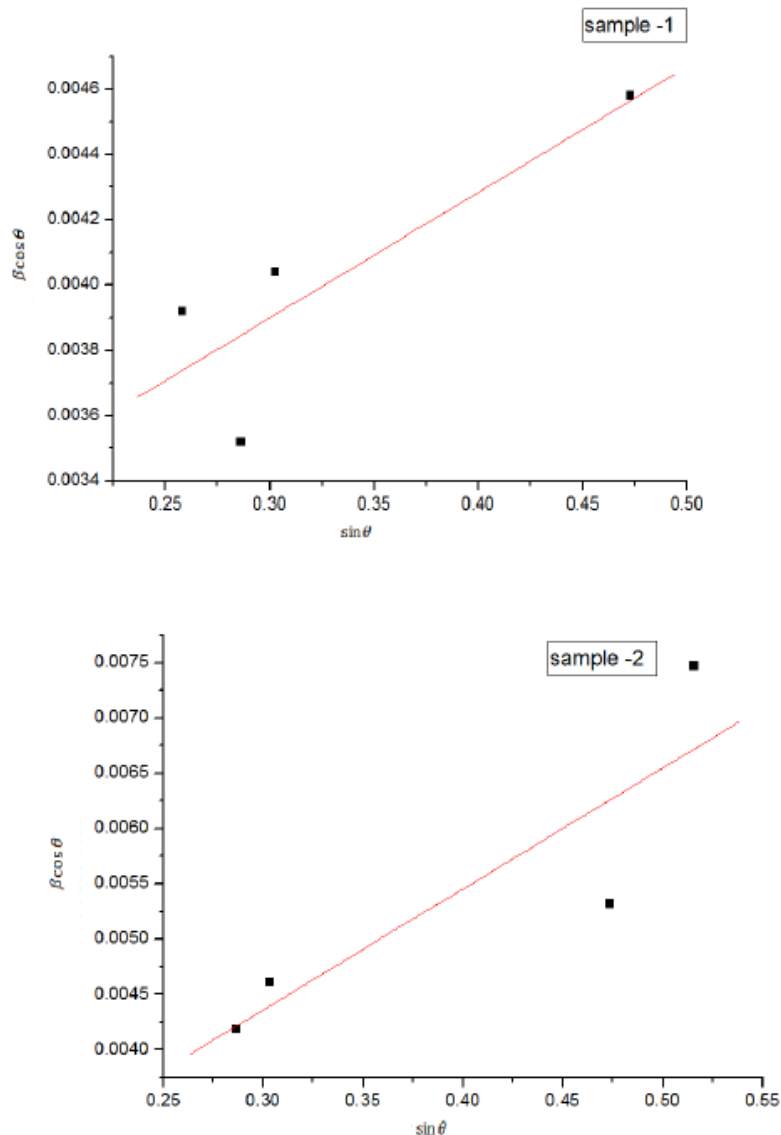
If both contributions are present then their combined effect should be determined by convolution. The simplification of Williamson and Hall is to assume the convolution is either a simple sum or sum of squares. Using the former equations we get

$$\beta_{tot} = \beta_e + \beta_L = C\epsilon \tan \theta + \frac{K\lambda}{L \cos \theta}$$

If we multiply this equation by $\cos \theta$ we get,

$$\beta_{tot} \cos \theta = C\epsilon \sin \theta + \frac{K\lambda}{L}$$

Comparing this to the standard equation for a straight line (m=slope: c= intercept) $y=mx+c$. We see that by plotting $\beta_{tot} \cos \theta$ versus $\sin \theta$; we obtain the strain component from the slope ($C\epsilon$) and the size component from the intercept ($K\lambda/L$). Such a plot is known as a Williamson-Hall Plot. The assumptions of this method are its absolute values should not be taken too seriously but it can be a useful method if used in a relative sense; for example a study of many powder patterns of the same chemical compound, but synthesized under different conditions, might reveal trends in the crystalline size/strain which in turn can be related to the properties of the product. Fig. 4 shows Williamson Hall Plot.



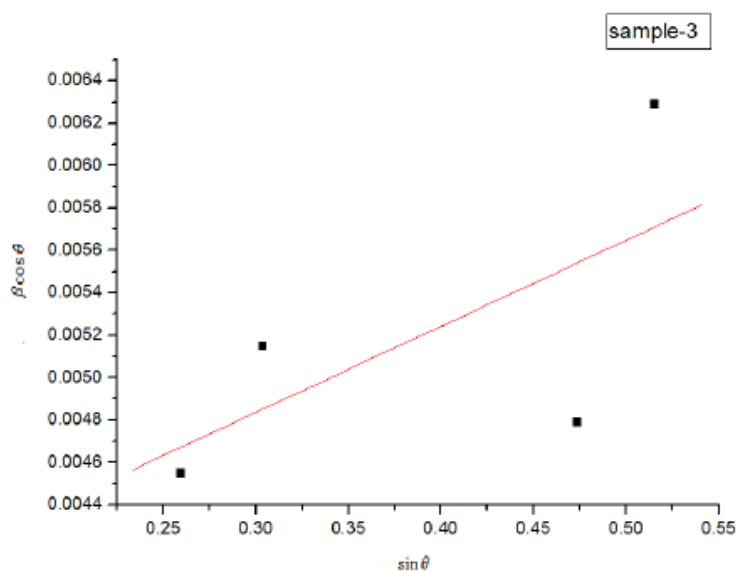


Fig 4. Williamson Hall plots of three samples.

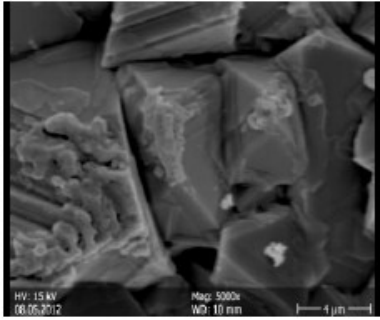
2.5 SEM Analysis

Scanning Electron Microscope is employed to record and analyze the surface morphology of the prepared samples. The SEM micrographs shown below gives an average grain size of 10 μ m. The surface morphology indicates the well formed samples with almost uniform well defined grains. It is found that the average grain diameter remains almost same with Ti concentration. Table 1 presents approximate particle size of the three samples

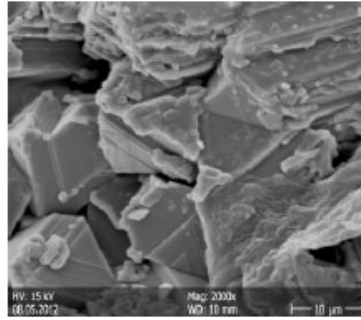
Table 1. Grain size of MnZnTiFeO from SEM Analysis

Sample	Particle Size(μ m)
$Mn_{0.9} Zn_{0.2} Ti_{0.1} Fe_{1.8} O_4$	8
$Mn_{0.95} Zn_{0.2} Ti_{0.15} Fe_{1.7} O_4$	10
$Mn_1 Zn_{0.2} Ti_{0.2} Fe_{1.6} O_4$	10

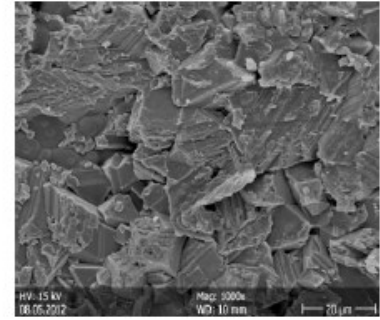
Sample - 1



(a1)

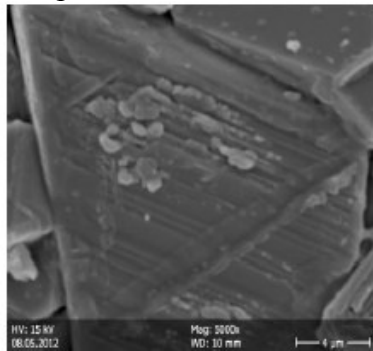


(a2)

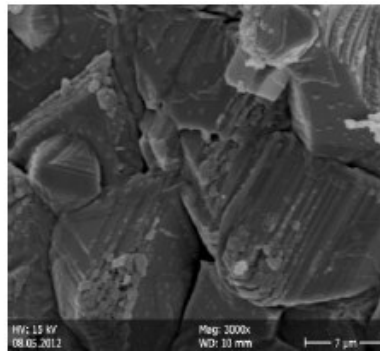


(a3)

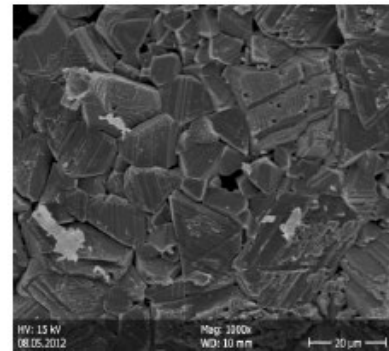
Sample- 2



(b1)

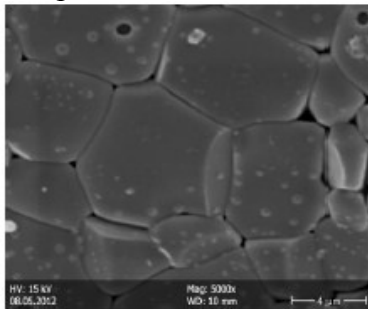


(b2)

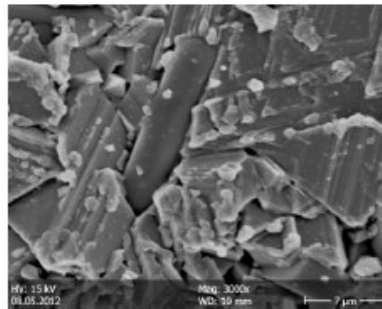


(b3)

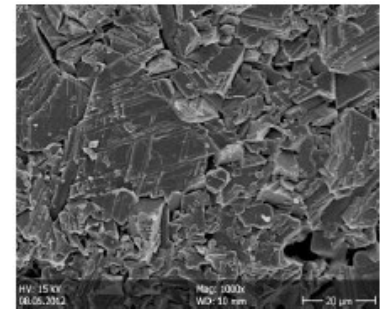
Sample-3



(c1)



(c2)



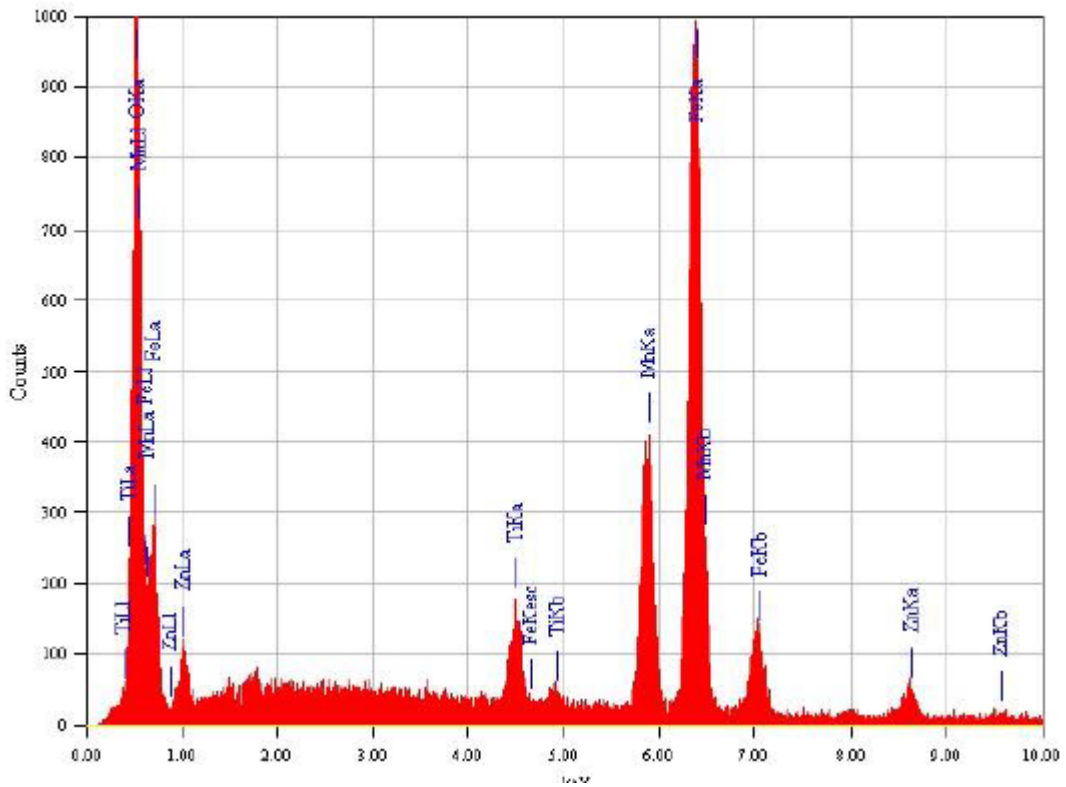
(c3)

Fig 5. SEM Photographs of the samples

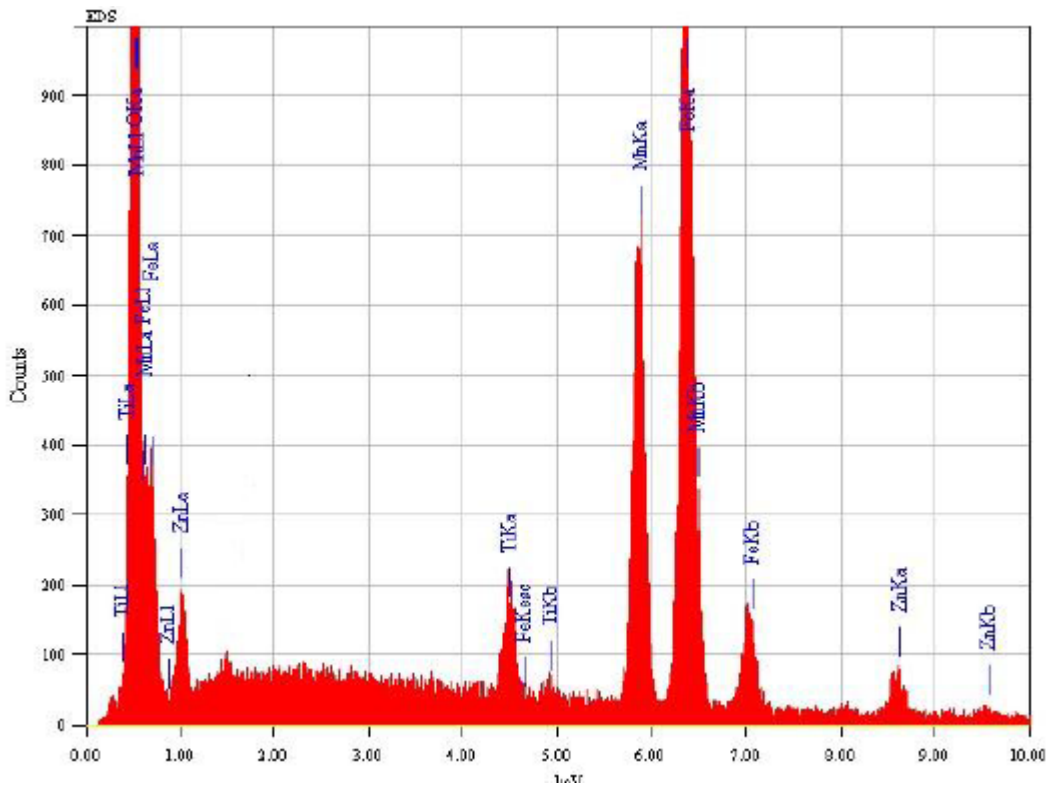
2.6 Energy Dispersed X Ray Spectrograph (EDX)

The instrument used for this measurement is ISIS Link Oxford Instrument UK. EDX shows the composition details of the prepared powder. Here an electron beam of 10-20 keV strikes the surface of a sample which causes X-ray to be emitted from point of incidence. The energy of the X-ray from different elements is different and gives the presence of a particular element. When an X-ray strikes the detector, photoelectrons are emitted which in turn generates electron-hole pairs. In this method elements with low atomic number are difficult to be detected. Figure (6) shows the EDX of three samples. Table 2 presents the material content of the samples.

Sample-1



Sample-2



Sample-3

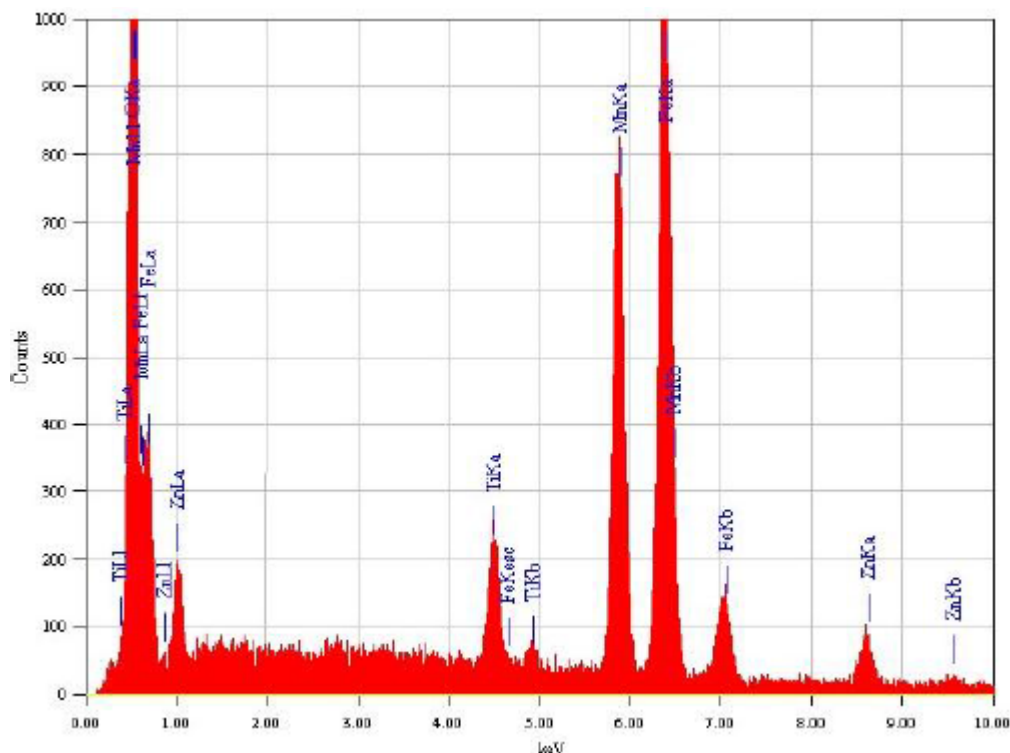


Fig 6. EDX of the samples

Table 2. Material content of the samples (EDX)

Material	Sample 1	Sample 2	Sample 3
	%	%	%
O	36.4	39.49	37.98
Ti	2.99	3.46	4.55
Mn	13.35	17.21	19
Fe	43.27	35.49	33.19
Zn	4	4.36	5.28

3. Results and Discussion

XRD Spectrum for the different Titanium concentrations of the sample gave a clear idea about the maximum intensity peak shifting of different concentrations of the sample. As the Ti concentration increases the highest peak shifts from left to right with decreasing intensity. The peaks are identical to the peaks of MnZn ferrites and hence the samples are of single phase spinel structure with $a=8.445$. Lattice parameter increases with Titanium concentration. It is due to the increase in ionic radius of titanium. Thus it evidently shows that Ti^{3+} goes in the octahedral site by replacing Fe^{3+} .

From Fig (1) the peak broadening in the XRD pattern clearly indicated the nature of the very small crystals. Figure 2 shows that lattice parameter varies with titanium concentration. Diffraction pattern will show broadening because of particle size and strain. The observed line broadening (figure 3) is used to estimate the average size of the particles and is found to be around $10\mu m$. From the Williamson Hall Plot (Fig. 4) we get a study of many powder patterns of the same chemical compound, but synthesized under different conditions, might reveal trends in the crystalline size/strain which in turn can be related to the properties of the product.

Fig (5) shows the SEM image of MnZnTiFeO. SEM photographs revealed the maximum dimensions of the particles remains almost same. This is an experimental proof of the theoretical calculation of particle size and found to be around $10\mu m$.

EDX spectrum of MnZnTiFeO gave the information on the elemental composition of the material. The elemental compositions agree with the stoichiometric relations of the prepared compound. The EDX spectra Fig (6) obtained give the material under investigation. From the EDX spectrum of the samples peak positions at 0.637 keV and 5.894 keV correspond to $L\alpha$ and $K\alpha$ lines of Mn as reported in the EDAX International chart. Similarly at 1.012 keV and 8.630 keV we get $L\alpha$ and $K\alpha$ lines of Zn. At 0.452 keV and 4.508 keV we get $L\alpha$ and $K\alpha$ lines of Ti. At 0.705 keV and 6.398 keV we get $L\alpha$ and $K\alpha$ lines of Fe. Also at 0.52 keV we get $K\alpha$ line of Oxygen atom. Hence the dominant peak positions correspond quite well to the energy pattern of the corresponding materials such as Mn, Zn, Fe, Ti and O reported in the EDAX International chart. Table 2 shows the percentage of elements in the prepared samples.

The size and strain of the experimentally observed broadening of several peaks are computed simultaneously using least squares method. When particle size becomes smaller, due to size effect, the peaks become broad and widths larger. The broadening of peak may also occur due to micro strains of the crystal structure arising from defects like dislocation and twinning[9]. Here, Williamson-Hall plot is plotted with $\sin \theta$ on the x-axis and $\beta \cos \theta$ on the y-axis (in radians). A linear fit is got for the data. From this fit, particle size and strain are extracted from Y intercept and slope respectively. The extracted particle size is 10 μ m and strain is 0.00125 from Williamson Hall plot (Fig.4).

The full width at half maximum was extracted using X' pert High score plus program. A clear change was observed in FWHM of XRD diffractograms, which was reflected in the calculations of the crystalline sizes. It was found that the average crystalline size remains as same with the increase in concentration of Ti. The result is in consistent with the results obtained for the lattice parameters where increasing the lattice parameter may results in increase in total crystalline sizes[10]. Similar results were reported for other spinal ferrites and ferroelectric materials[11].

4. Conclusion

Ti⁴⁺ ions substituted Manganese-Zinc ferrites were prepared successfully by the conventional solid state reaction method and characterized by XRD, SEM, EDX and particle measurement. XRD data confirmed the formation of spinel ferrites. At low substitution level (x=0.1) the Ti⁴⁺ ions enter the spinel lattice on the vacant octahedral B-sites, which leads in the increase of lattice parameter and saturation magnetization. But the saturation magnetization decreases in B-sublattice due to the dilution of Fe³⁺. Increasing of Ti substitution forces the Fe³⁺ ions to redistribute in A-sublattice (tetrahedral sites) in place of Mn²⁺ ions. This causes steep decrease in the saturation magnetization as Ti substitution increases. The increase in lattice parameter is due to the increase in ionic radius of titanium. Thus it evidently shows that Ti³⁺ goes in the octahedral site by replacing Fe³⁺. SEM studies revealed that the average grain size of samples is 10 μ m. EDX spectrum shows the elements of the sample and it agree with stoichiometric relations of the prepared sample. The value of particle size calculated from the Williamson-Hall plot method is in agreement with that of the particle size measured from other methods.

Acknowledgements

The authors are thankful to the Principal, CMS College, Kottayam and Director, Centre for Condensed Matter, CMS College, Kottayam for providing the facilities in the laboratories.

References

- [1] J.Smit and H.P.J.Wijin, Ferrites, John Wiley and Sons, New York (1959)
- [2] W.H.Bragg, Nature, 95, 561, (1915)
- [3] M.Arumugam, Material Science, Anuradha Agencies Publishers, Vidyal karupur, Madras (1987)
- [4] P.Tarte, Acta Cryst, 16b, 227 (1963)
- [5] G.Srinivasan, Phy.Chem.Solids, 57, K179 (1980)
- [6] E.P Wohlfarth, Ferro.Mag.Mat, North Holland, Amsterdam 3(4), 191 (1982).
- [7] West.A.R (1974), Solid state Chemistry and its Applications. Wiley, New York.
- [8] Williamson. G.K and Hall. W H (1953), X-Ray Line Broadening from Filled Aluminium and Wolfram. Acta Metallurgica 1.22-31. [http://dx.doi.org/10.1016/0001-6160\(53\)90006-6](http://dx.doi.org/10.1016/0001-6160(53)90006-6)
- [9] Ghosh.S.C, Thanachayanont.C and Dutta.J (2004), Studies on Zinc Sulphide Nanoparticles for Field Emission Devices. The 1 st ECTI Annual conference (ECTI-CON 2004), Pattaya, 13-14 May 2004, 145-148.
- [10] Nasser.Y.Mostafa, M.M Hessien, Abdallah A. Shaltout, J. Alloys Compou
- [11] U.Ghazanfar, S.A.Siddiq, G.Abbas, Mater.Sci, Eng.B 118(2005)132.